

Evaluation of Molecularly Imprinted Polyurethane as an Optical Waveguide for PAH Sensing

Yin-Chu Chen^a, Jennifer J. Barzier^b, Mingdi Yan^b, Scott A. Prahl^a

^aDepartment of Biomedical Engineering, OHSU, Portland, OR

^bDepartment of Chemistry, PSU, Portland, OR

ABSTRACT

We developed a numerical model for the fluorescence output efficiency of a molecularly imprinted polymer (MIP) waveguide sensing system. A polyurethane waveguide imprinted with a polycyclic aromatic hydrocarbon (PAH) molecule was fabricated using micromolding in capillaries. The coupling of light into a 5 mm long MIP segment was verified by comparing the output transmission signals of a deuterium lamp from the MIP waveguide collected by an optical fiber with the background lamp signals collected by the same optical fiber. It was found that polyurethane MIP was an effective waveguide but absorbed much shorter wavelengths, especially in the UV region, thereby the transmission of light appeared orange/red in color. The high background absorption of polyurethane in the spectrometric regions of interest was found to be a critical problem for sensor sensitivity. Our numerical model shows that the fluorescence output is only 2×10^{-6} of the input excitation for 25 mM anthracene for a 5 mm polyurethane waveguide. A 10 fold decrease of background absorption will increase the fluorescence output 250 times.

Keywords: polycyclic aromatic hydrocarbon, molecularly imprinted polymers, optical fiber sensor, light coupling efficiency

1. INTRODUCTION

Evanescent-wave fluorescence-based fiber-optic biosensors detect the binding of an antigen to an antibody immobilized in the distal end of an optical fiber.¹⁻⁴ Detected refractive index changes caused by binding of an antigen and an antibody are limited to the evanescent sensing region (typically less than $1 \mu\text{m}$ thick). For immunoassay recognition elements, this is an advantage because fluorophores outside the evanescent field don't contribute to the emission signal. Molecularly imprinted polymer techniques allow much greater detection volumes that may capture more analytes. For instance, a $600 \mu\text{m}$ fiber coated for 5 cm with MIP with an active sensing depth of $1 \mu\text{m}$ will have a detecting volume of $\sim 10^{-2} \text{mm}^3$. On the other hand, if the fiber itself is a MIP, which acts as both a detecting element and a waveguide, a $100 \mu\text{m} \times 100 \mu\text{m} \times 1 \text{cm}$ long MIP waveguide will have 10 times more detecting volume than an evanescent-wave sensor. Another advantage is that the light intensity inside a MIP waveguide that directly excites the analytes is stronger than that in the evanescent field (which decays exponentially). Yet another advantage is that a greater proportion of the fluorescence signal, generated inside the MIP, will be guided directly to the output. A potential problem of a MIP waveguide, however, is the attenuation of the signals due to the background absorption of polymers, and an increase in the equilibrium time of the analytes and MIP.

The concept of using the biochemical sensing layer itself as an optical waveguide was presented by Hisamoto *et al.*⁵ They used an "active polymer-waveguide platform" where the sensing layer also acted as the guiding layer. The poly(vinylchloride) membrane was used both as a sensing layer and as the evanescent-wave waveguide core layer. The absorbance signal was measured, and the sensitivity of such a system was shown to be greater than that in the evanescent-wave sensing mode. Although optical sensors based on molecularly imprinted polymers have been constructed,⁶⁻¹⁰ few publications have used MIPs directly as an optical waveguide.¹¹ For biochemical sensing use, the attenuation of light may not be as critical as an optical fiber for optical communications.

Further author information: (Send correspondence to S. A. P.)

Y.-C. C.: E-mail: yinchu@bme.ogi.edu, Tel: (503) 216-6830

S. A. P.: E-mail: prahl@bme.ogi.edu, Tel: (503) 216-2197

We developed a theoretical model for the fluorescence output efficiency of a MIP waveguide. A MIP system, polyurethane imprinted with polycyclic aromatic hydrocarbon (PAH) molecule, was evaluated based on the polymer's optical properties. Based on this theoretical model, the optimal optical properties of MIP was suggested to increase the sensitivity of MIP used as an optical waveguide.

2. THEORY

2.1. Theoretical Model of Output signals of a MIP Waveguide

In this model, the analytes are assumed to be homogeneously distributed within the MIP; reabsorption and scattering events are neglected. The analyte and the polymer have absorption at excitation wavelength λ_x and fluorescence at wavelength λ_m . The background (polymer) absorption coefficient at λ_x is μ_a^x , the absorption coefficient of the analytes is μ_a^f , and the background absorption coefficient of emitted fluorescence light λ_m is μ_a^m . The schematic representation of this model is shown in Fig. 1.

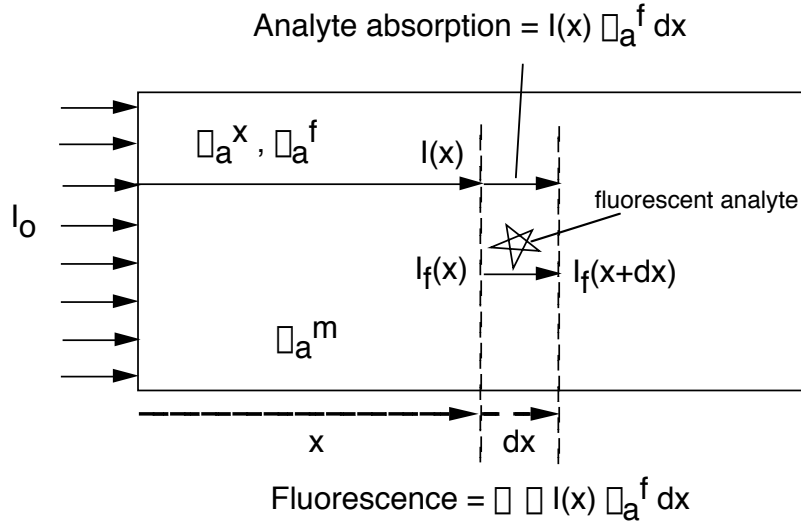


Figure 1. The schematic representation of MIP-waveguide model.

If the incident irradiance is I_0 at the input end, the irradiance at a distance x from the input end becomes

$$I(x) = I_0 e^{-(\mu_a^x + \mu_a^f)x} .$$

Assuming the irradiance of the emitted fluorescence light λ_m at x is $I_f(x)$, the irradiance drops to $I_f(x)\mu_a^m dx$ at $x + dx$ because of the background absorption. Since both the analyte and the polymer fluoresce, assume the fluorescence quantum yield is Φ_a for analyte and Φ_p for polymer and the fluorescence irradiance from the analyte is I_f and from the polymer is I_p . We consider the fluorescence from the analytes first. The irradiance absorbed by the analytes for fluorescence in dx distance is $I(x)\mu_a^f dx$. Analytes release a portion (the quantum Yield, Φ_a) of the absorbed energy as fluorescent light λ_m , and only some fraction (η) will propagate to the output end of fiber, so the newly fluorescent light from the analyte added to $I_f(x + dx)$ is $\eta\Phi_a I(x)\mu_a^f dx$. Therefore, the analyte fluorescence irradiance at position $(x + dx)$ becomes

$$I_f(x + dx) = I_f(x) - I_f(x)\mu_a^m dx + \eta\Phi_a I(x)\mu_a^f dx.$$

Solving this equation for $I_f(x)$ with an initial condition $I_f(0) = 0$, we get the output irradiance relative to the input irradiance I_0 for fluorescence from the analytes (called "relative output efficiency" Q_a) as

$$Q_a = \frac{I_f(x)}{I_0} = A \left[e^{-\mu_a^m x} - e^{-(\mu_a^x + \mu_a^f)x} \right] , \quad (1)$$

where

$$A = \frac{\eta\Phi_a\mu_a^f}{\mu_a^x + \mu_a^f - \mu_a^m} .$$

Similarly, the relative output efficiency for background fluorescence (from the polymer itself) (Q_p) is derived as

$$Q_p = \frac{I_p(x)}{I_0} = A \left[e^{-\mu_a^m x} - e^{-(2\mu_a^x)x} \right] , \quad (2)$$

where

$$A = \frac{\eta\Phi_p\mu_a^x}{2\mu_a^x - \mu_a^m} .$$

3. MATERIALS AND METHODS

3.1. Materials

Polyurethane imprinted with anthracene, a polycyclic aromatic hydrocarbon (PAH) molecule, was made from a mixture of 1.25 M solutions of monomers composed of 0.375 mmol bisphenol A (Aldrich) and 0.455 mmol p,p'-diisocyanatodiphenylmethane (Merck-Schuchardt, Hohenbrunn, Germany); crosslinkers composed of 0.250 mmol trihydroxybenzene and 0.195 mmol p,o,p'-triisocyanatodiphenylmethane (Merck-Schuchardt, Hohenbrunn, Germany) in dimethylformamide (DMF)^{12,13}; and the imprint molecule anthracene (Aldrich) at 25 mM in dimethylformamide (DMF).

3.2. MIP waveguide preparation

Waveguides were fabricated using the technique of micromolding in capillaries (MIMIC) as shown in Fig. 2.¹² A silicon master pattern made up of lines (50 μm in height by 50 μm in width and 7.5 cm in length) was fabricated through conventional photolithography using SU-8 photoresist (Microchem Corporation, Newton, MA). The PDMS mixture was poured over this master pattern and allowed to cure at 70°C for 4 hours. The PDMS stamp was then peeled off; thereby creating a negative image of the original pattern. The ends of the stamp were then carefully cut with a razor blade to open up the channels and each stamp was cleaned via sonication in ethanol. When placed on a silicon wafer, the stamp formed small microchannels that were filled with an imprinting solution by capillary action. The silicon wafers were previously cleaned in piranha solution (3:1 v/v, conc. H_2SO_4 / 30% H_2O_2) and were silanized with 3-aminopropyl trimethoxysilane in order to ensure covalent attachment of the polymer to the substrate.¹⁴ Subsequent overnight polymerization under ambient conditions and stamp removal left behind imprinted filaments attached to the wafer support. Filaments were visually inspected via an optical microscope (Olympus BHM).

3.3. Light coupling and relative transmission measurements

A quartz lens with a focal length of 2 cm was used to focus the light from the deuterium lamp into the waveguide. Coupling was verified when the distal end of the waveguide lit up. The waveguide was rotated to an angle of approximately 30° relative to the optical axis such that the direction of the light emitted from the fiber was distinct from the illumination light. The light coming out from the distal end of MIP waveguide was then coupled into a 400 μm optical fiber and recorded by a Fluorolog-3 spectrofluorimeter. The relative four positions of the focus of the light and the optical fiber were illustrated in figure 3. First, the focus of the light is at the tip of MIP waveguide, position L1. The collecting optical fiber was then put in position A where the light was directly emitted from the lens (approximately 3 mm away from the tip of MIP waveguide). This served as the reference background signal. Second, the optical fiber was moved to position B to collect the light coming out from MIP waveguide. Third, the focus of the light was moved to focus to the side of MIP waveguide, position L2, but the angle remained the same. The optical fiber remained in position B. Finally, the optical fiber was moved to position A again.

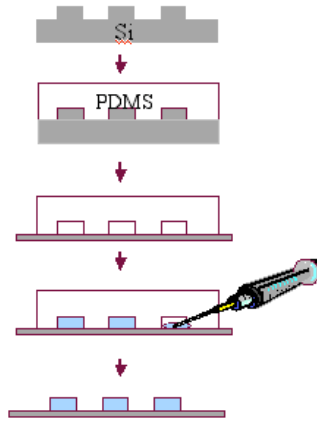


Figure 2. The micromolding in capillaries technique steps are to (1) create master mode, (2) pour and cure PDMS, (3) remove PDMS and place PDMS on silicon wafer with thin coat of PDMS, (4) fill channels with MIP and allow to polymerize, and (5) peel PDMS away.

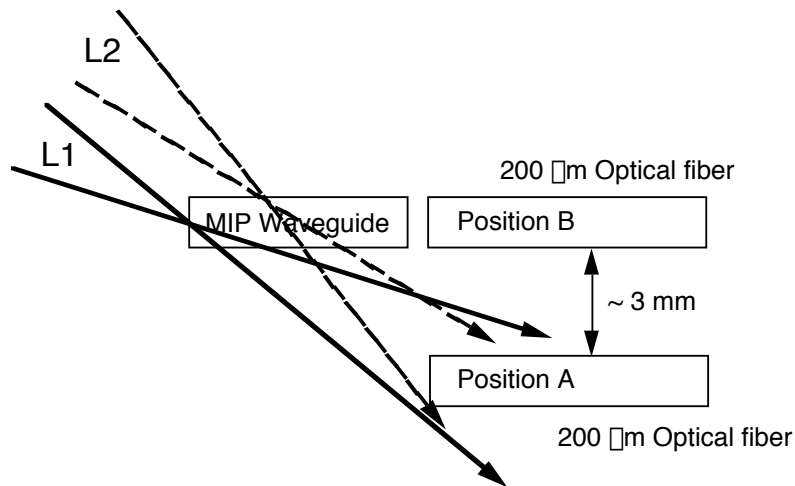


Figure 3. The relative four positions of the focus of the light and the optical fiber. Two positions of the focus of light: position L1: the focus of the light is at the tip of MIP waveguide; position L2: the focus of the light was moved to the side of MIP waveguide. Two positions of the optical fiber: position A: the collecting optical fiber was put in the position where the light was directly emitted from the lens, approximately 3 mm away from the tip of MIP waveguide; position B: the optical fiber was at the tip of MIP waveguide to collect the light coming out from MIP waveguide.

1. The ratio of transmission of light through MIP waveguide to the background:

$$T_{mip} = \frac{\text{light focus at L1 and fiber collect at B}}{\text{light focus at L1 and fiber collect at A}}$$

2. The comparison data:

$$T_{side} = \frac{\text{light focus at L2 and fiber collect at B}}{\text{light focus at L1 and fiber collect at A}}$$

3. The background of focus to the tip to the background of focus to the side:

$$T_{background} = \frac{\text{light focus at L2 and fiber collect at A}}{\text{light focus at L1 and fiber collect at A}}$$

4. RESULTS AND DISCUSSION

4.1. Light coupling and relative transmission measurements

Figure 4 shows the raw transmission spectra of the four measurements and their relative transmission spectra, T_{mip} , T_{side} and $T_{background}$. The L1-A and L2-A curves showed that similar background spectra were collected at position A, which is 3 mm away to waveguide output tip, for both focusing the light to the MIP tip and focusing to the side of MIP. The transmission at longer wavelengths, above 600 nm, is about 1.5 times higher than the wavelengths between 350 nm to 600 nm. This suggests that the light between 350 nm to 600 nm is slightly absorbed when passing through MIP waveguide, but since the waveguide is only 100 μm thick, the amount absorbed is only $\sim 5\%$.

The T_{side} curve shows that about 10 times more light than $T_{background}$ was collected. According to Fresnel equations, no light going into MIP from position L2 is totally internal reflected, therefore little light will be guided by MIP waveguide. If we collected any signals, that would be the light scattered by the silicon substrate, MIP or dust.

The T_{mip} (red) curve is much higher than the other two, which demonstrates that MIP was an effective waveguide. The total output intensity was the light guided by the MIP waveguide (since any incident angle (focusd at L1 position) on the MIP waveguide will be guided due to the total internal reflection when assuming the refractive index of MIP is 1.5) plus the light scattered from the substrate, MIP or dust (the relative amount was shown by T_{side}). The T_{mip} curve shows that the transmission above 650 nm is twice higher than the wavelength below 550 nm. This means that those with shorter wavelengths are absorbed more when they propagate through MIP.

4.2. Numerical simulation of MIP relative output efficiency Q

In the following numerical tests, the proportion (η) of fluorescence light that propagates to the output end of waveguide is assumed 0.25 since the fluorescence light is equally distributed to all direction (isotropic) and the part from solid angle $-\pi/2$ to $+\pi/2$ among 4π is assumed to propagate to the output end.

For anthracene imprinted polyurethane MIP system, the quantum yield is 4×10^{-3} for 25 mM anthracene in MIPs, and 5×10^{-4} for polyurethane itself.¹³ The optical properties of MIPs are $\mu_a^x = 30 \text{ cm}^{-1}$ at 362 nm and $\mu_a^m = 12 \text{ cm}^{-1}$ at 404 nm, and the absorption coefficient of 25 mM anthracene in MIPs is $\mu_a^f = 190 \text{ cm}^{-1}$ at 362 nm excitation.¹³ The relative output efficiency Q_a and Q_p as a function of waveguide length was plotted in Fig. 5. As we can see, MIP has a maximum Q_a value of 0.07% at length 0.14 mm, and Q_a drops exponentially as the length of the MIP waveguide increases due to the high background absorption of polymers. The relative output efficiency Q_a is only 0.0002% for 5 mm MIP waveguide. If the polymer's background absorption drops 10 times, a 0.26 mm waveguide will have a maximum Q_a of 0.09% and the Q_a only drops slightly, thus 5 mm MIP will have Q_a up to 0.05%.

For the ratio of the background polymer fluorescence to the analyte fluorescence (S/N ratio = Q_a/Q_p), MIP has higher S/N ratio for shorter length of waveguide (Fig. 6). For anthracene imprinted polyurethane system, the S/N ratio drops quickly in the beginning ($< 0.25 \text{ mm}$) and plateaus at a value around 11 for waveguide

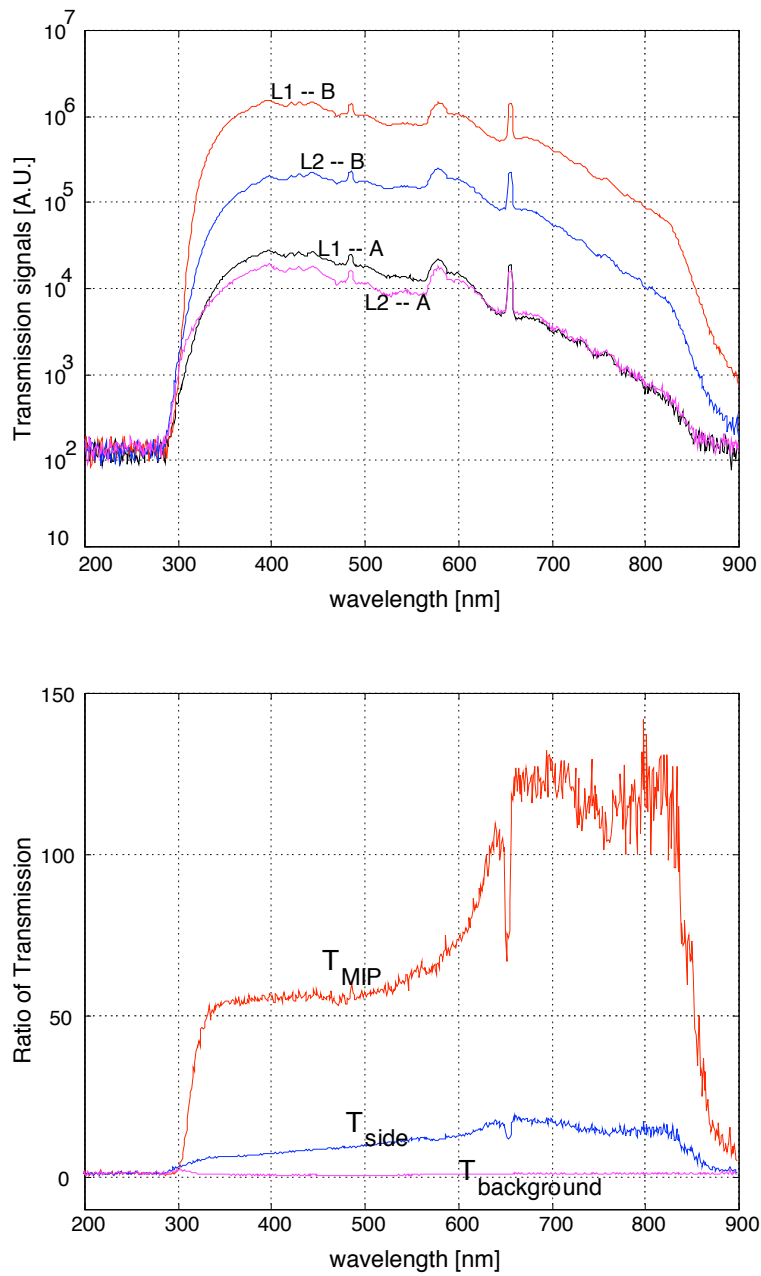


Figure 4. Top figure is the transmission spectra of the four measurements. Bottom figure is the ratio of the transmission spectrum. The magenta curve is $T_{background}$. The blue curve is T_{side} . The red curve is T_{MIP} .

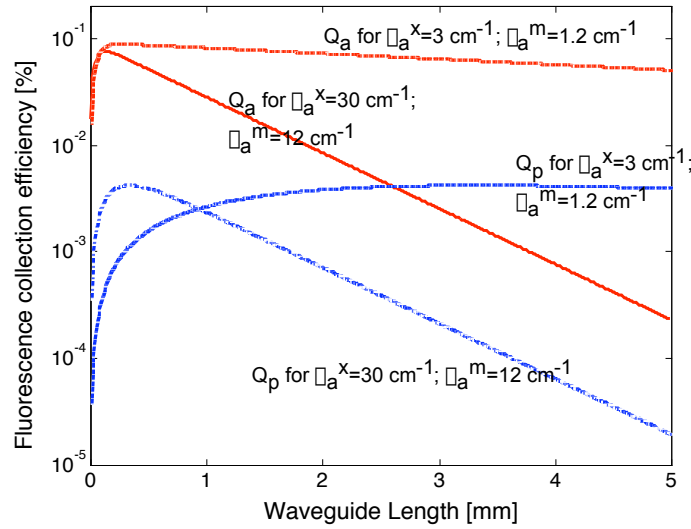


Figure 5. Numerical results of the relative output efficiency for analyte fluorescence Q_a and for polymer fluorescence Q_p as a function of MIP waveguide length.

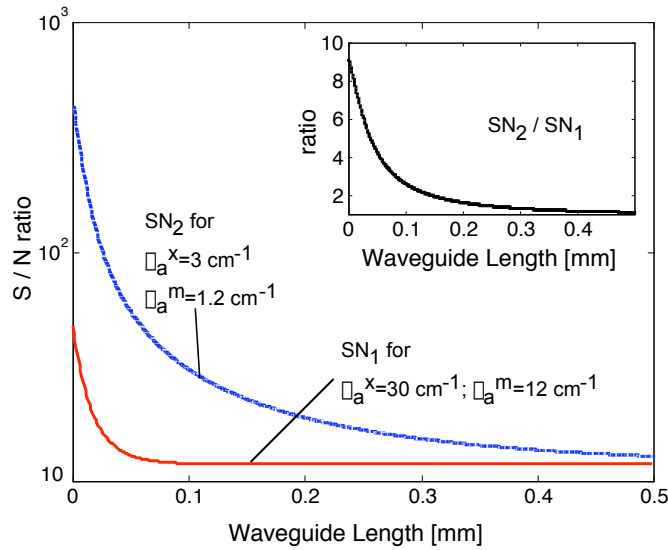


Figure 6. The signal to noise ratio (Q_a/Q_p) of a MIP waveguide as a function of waveguide length.

lengths longer than 0.5 mm (the solid line, SN_1 , in Fig. 6). If a polymer's background absorption drops 10 times (the dashed line, SN_2 , in Fig. 6), the S/N ratio is more than 5 times higher than SN_1 for waveguides shorter than 0.02 mm. However, the SN_2 drops to a value close to SN_1 as the waveguide length increases to 0.5 mm (sub-figure in Fig. 6).

5. CONCLUSIONS

This study combines micromolding in capillaries (MIMIC) and MIP technique to fabricate imprinted optical waveguides for the detection of fluorescent polyaromatic hydrocarbon (PAH) molecules. Coupling of light into 5 mm long waveguide segments was verified through the comparison of relative transmission measurements. This

suggests that a novel optical sensor using MIP (as the recognition element) as an optical waveguide is possible. However, our numerical simulation shows that the relative output efficient is only 2×10^{-6} for 25 mM anthracene due to the high polymer absorption in the spectrometric regions of interest. A ten fold decrease of background absorption will increase the fluorescence output efficiency 250 times for a 5 mm waveguide segment.

Therefore, modifications in the type and purity of polymers may lead to future waveguides capable of light propagation as well as analyte detection. The emitted fluorescence from the analytes can be measured and calibrated according to analyte concentrations as long as the excitation and emission wavelength of the analytes are not at wavelengths that are strongly absorbed by the polymer. In this way, the sensing volume of MIPs can be increased, which may increase the sensitivity. Furthermore, if a single MIP waveguide can be successfully used as a biochemical sensor, by combining it with the MIMIC technique, an array of MIPs may be fabricated on a single chip to allow simultaneous analysis of multiple analytes.

ACKNOWLEDGMENTS

This work was supported by National Institute of Health Grant NIH-CI-R24-CA84587-04.

REFERENCES

1. U. Narange, G. P. Anderson, F. S. Ligler, and J. Burans, "Fiber optic-based biosensor for risin," *Biosens. Bioelectron.* **12**, pp. 937–945, 1997.
2. A. P. Abel, M. G. Weller, G. L. Duveneck, M. Ehrat, and H. M. Widmer, "Fiber-optic evanescent wave biosensor for the detection of oligonucleotides," *Anal. Chem.* **68**, pp. 2905–2912, 1996.
3. E. A. James, K. Schmeltzer, and F. S. Ligler, "Detection of endotoxin using an evanescent wave fiber-optic biosensor," *Appl. Biochem. and Biotech.* **60**, pp. 189–201, 1996.
4. L. K. Cao, G. P. Anderson, F. S. Ligler, and J. Ezzell, "Detection of Yersinia pestis Fraction 1 antigen with a fiber optic biosensor," *J. Clin. Microbio.* **33**, pp. 336–341, 1995.
5. H. Hisamoto, K. H. Kim, Y. Manabe, K. Sasaki, H. Minamitani, and K. Suzuki, "Ion-sensitive and selective active waveguide optodes," *Anal. Chim. Acta* **342**, pp. 31–39, 1997.
6. D. Kriz, O. Ramstrom, A. Svensson, and K. Mosbach, "Introducing biomimetic sensors based on molecularly imprinted polymers as recognition elements," *Anal. Chem.* **71**, pp. 4559–4563, 1999.
7. F. L. Dickert and M. Tortschanoff, "Molecularly imprinted sensor layers for the detection of polycyclic aromatic hydrocarbons in water," *Anal. Chem.* **71**, pp. 4559–4563, 1999.
8. A. L. Jenkins, O. M. Uy, and G. M. Murray, "Polymer-based lanthanide luminescent sensor for detection of the hydrolysis product of the nerve agent soman in water," *Anal. Chem.* **71**, pp. 373 – 378, 1999.
9. P. Turkewitsch, B. Wandelt, G. D. Darling, and W. S. Powell, "Fluorescent functional recognition sites through molecular imprinting. A polymer-based fluorescent chemosensor for aqueous cAMP," *Anal. Chem.* **70**, pp. 2025 – 2030, 1998.
10. R. Levi, S. McNiven, S. A. Piletsky, S. H. Cheong, K. Yano, and I. Karube, "Optical detection of chloramphenicol using molecularly imprinted polymers," *Anal. Chem.* **69**, pp. 2017 – 2021, 1997.
11. M. Yan and A. Kapua, "Fabrication of molecularly imprinted polymer microstructures," *Anal. Chim. Acta.* **435**, pp. 163–167, 2001.
12. J. J. Brazier, M. Yan, S. A. Prahl, and Y.-C. Chen, "Molecularly imprinted polymers used as optical waveguides for the detection of fluorescent analytes," in *Molecularly Imprinted Materials Sensors and Other Devices*, K. J. Shea, M. J. Roberts, and M. Yan, eds., **723**, pp. 115–120, Materials Research Society Symposium Proceedings, 2002.
13. Y.-C. Chen, J. J. Brazier, M. Yan, P. R. Bargo, and S. A. Prahl, "Fluorescence-based optical sensor design for molecularly imprinted polymers," *Sens. Actuators, B – Chem.* **102**, pp. 107–116, 2004.
14. D. A. Stenger, J. H. Georger, C. S. Dulcey, J. J. Hickman, A. S. Rudolph, T. B. Nielsen, S. M. McCort, and J. M. Calvert *J. Am. Chem. Soc.* **114**, pp. 8435–8442, 1992.